

Investigation of the self-assembly of hydrophobic self-complementary ionic tetrapeptides

A. Desii · C. Duce · L. Ghezzi · S. Monti ·
R. Solaro · M. R. Tiné

AICAT2008 Conference
© Akadémiai Kiadó, Budapest, Hungary 2009

Abstract The self-aggregation of two short ionic tetrapeptides (RWDW and RVDV, where *R* = arginine, *V* = valine, *W* = tryptophan, *D* = aspartic acid) was studied by different experimental techniques such as, atomic force microscopy (AFM), light scattering (LS), isothermal titration calorimetry (ITC) and viscosimetry. AFM was used to investigate the morphology of the aggregates; the AFM images showed the presence of fibrillar aggregates whose number and length increased with increasing oligopeptides concentration. On the other hand, the collected experimental calorimetric and physical chemical results consistently indicated a critical aggregation concentration (*cac*) around 0.5 and 2.0 mM for RWDW and RVDV respectively.

Keywords Atomic force microscopy · Isothermal titration calorimetry · Oligopeptide · Self-assembly

Introduction

Molecular self-assembly, by definition [1] is the spontaneous organization of molecules under thermodynamic equilibrium conditions into structurally well-defined arrangements through a number of non-covalent interaction (which typically include hydrogen bonds, ionic bonds,

hydrophobic, and van der Waals' interactions). These molecules undergo self-association forming hierarchical structures without any external instruction. Although each bond is rather weak, the collective interactions can result in very stable structures.

There are many examples of molecular self-assembly in nature. Almost all biomolecules interact and self-organize to form well defined architectures that are associated with their functionality. Self-assembly is also central to many human diseases, viruses, for example, are themselves incredibly sophisticated self-assembly systems and many studies have revealed that several types of protein-related physiological disorders, such as Alzheimer's, Parkinson's, prion diseases are related to abnormal protein aggregation [2]. Using natural processes as a guide, molecular self-assembly has emerged as a new and powerful strategy in biomedical and pharmaceutical areas [3]. In particular, oligopeptide self-assembly has been demonstrated to have potential for diverse biomedical applications including tissue repair, drug delivery, and biological surface engineering [3, 4]. The use of self-assembling oligopeptides presents several advantages; indeed, the basic units show excellent physiological compatibility and minimal cytotoxicity. Moreover, they are simple to design, extremely versatile and easy to synthesize, so that they can be tailored to specific needs.

Among self-assembling oligopeptides, the class of ionic self-complementary oligopeptides is of special interest [5]. This family of oligopeptides has repeating units of positively and negatively charged residues separated by hydrophobic residues. This structural feature allows for the formation of stable aggregates under particular conditions (pH, concentration, ionic strength) stabilized by complementary ionic bonds between different chains and intermolecular hydrophobic interaction in addition to conventional backbone

A. Desii · C. Duce · L. Ghezzi · R. Solaro · M. R. Tiné (✉)
Department of Chemistry and Industrial Chemistry,
University of Pisa, Via Risorgimento 35, 56126 Pisa, Italy
e-mail: mrt@dcci.unipi.it

S. Monti
Istituto per i Processi Chimico-Fisici (IPCF-CNR),
Area della Ricerca, via G. Moruzzi 1, 56124 Pisa, Italy

hydrogen bonding. One member of this family, EAKA16–II oligopeptide, was originally found as a repeated segment in a yeast protein. Its self-complementarity is distinctive in that it forms an insoluble macroscopic membrane upon salt addition [5]. This event can have implications for biomaterials and is a model for studying the insoluble oligopeptides found in some neurological disorders [5–7]. Since the discovery of EAKA16–II, extensive efforts were aimed at understanding and taking advantage of the self-assembly of this oligopeptide class. Despite the richness of ionic self-complementary oligopeptides reported in literature, very few physical chemical studies limited to AFM, surface tension and light scattering measurements have been reported on these systems. In this work we take into account some short self-complementary oligopeptides as models of longer peptides and protein aggregation. In particular the self-aggregation behaviour was studied by using atomic force microscopy (AFM), light scattering (LS), isothermal titration calorimetry (ITC), and viscosimetry. This study reports some very preliminary results of the self-aggregation of two tetrapeptides (RWDW and RVDV, where *R* = arginine, *V* = valine, *W* = tryptophan, *D* = aspartic acid), whose structures were planned by analogy with longer self-complementary oligopeptides, and it is a part of a wider project in which the structural factors affecting the self-assembling behaviour of ionic oligopeptides are considered through a multidisciplinary approach [8, 9]. Thus, if this preliminary study allowed to confirm that short peptides can form self-assembled structures, in the future we should further investigate the aspects of the aggregates' structure, including the secondary structure of the peptides, and predict the intra and intermolecular interactions which govern aggregation.

Experimental

Materials

RWDW and RVDV having chemical purity larger than 95% were purchased from Advanced ChemTech (Louisville, KY, USA) and stored at $-18\text{ }^{\circ}\text{C}$. The N-terminus and C-terminus were protected by acetyl and amide groups, respectively.

All reactants were analytical grade. Phosphate buffer (100 mM, pH 3.5) was prepared by dissolution of 0.00956 mol of KH_2PO_4 in 100 mL of H_3PO_4 4.26 mM. Phosphate buffer 50 mM was obtained from dilution of the 100 mM buffer.

Stock solutions were prepared by dissolving a weighed amount of tetrapeptide in 1–2 mL of ultrapure water and by adding the same volume of phosphate buffer solution (100 mM) at pH 3.5. When needed, stock solutions were filtered on 5.0 and/or 0.22 μm filters (Sartorius Stedim

Biotech GmbH, Gottingen, Germany). The proper standard solutions, required for the various measurements, were prepared by dilution of a stock solution.

Methods

pH measurements were made using a combined glass microelectrode (Hamilton, Biotrode 238140/05) in connection with an automatic Radiometer Analytical TIM 900 pH meter.

Absorption spectra were recorded between 200 and 400 nm by a Cary 50 UV–Vis spectrophotometer (Varian, Inc.).

A Perkin Elmer LS 50 spectrofluorimeter equipped with a xenon pulsed lamp was used for light scattering measurements. The excitation wavelength was 320 nm. The scattered light was collected at 90° with respect to the excitation wavelength between 310 and 330 nm, using quartz microcells of 10×2 mm (Helma GmbH & Co. KG, Müllheim, Germany).

Viscosity measurements were performed with an automated Micro Viscosimeter AMVn (Anton Paar GmbH) equipped with a 500 μL capillary. The results were expressed as specific viscosity ($\eta_{\text{sp}} = (\eta/\eta_0) - 1$, where η and η_0 are the viscosities of sample solution and solvent, respectively).

Isothermal titrations were performed by a Thermal Activity Monitor 2277 (Thermometric), equipped with a 612 Lund syringe pump and a 4 mL ampoule. Aliquots of 50 or 100 μL of $1.5 \div 2$ mM tetrapeptide solutions in 50 mM phosphate buffer were added to 2 mL of 50 mM phosphate buffer solution in 4 mL sample cell. All measurements were carried out at 298.15 K.

The atomic force microscope (AFM) probes the surface of a sample with a sharp tip, a couple of microns long and often $<100\text{ \AA}$ in diameter. The tip is located at the free end of a cantilever that is 100–200 μm long. Forces between the tip and the sample surface cause the cantilever to bend, or deflect. An optical lever detector measures the cantilever deflection as the sample is scanned under the tip via a piezoelectric tube. A proportional-integral (PI) controller is connected between the deflection detector and the piezoelectric tube displacing the sample. This controller causes the sample to move during the scan in a way that keeps constant a set-point value of a desired cantilever property (cantilever deflection in contact mode microscopy, cantilever oscillation amplitude in tapping mode microscopy). Thus, the correction signal sent by the controller to the piezoelectric tube can be interpreted as the sample topography.

Atomic force microscopy scanning of tetrapeptide aggregates was performed in tapping mode by using a Multimode AFM with Nanoscope IV controller (Veeco Metrology, Inc., Santa Barbara, CA, USA) equipped with

scanners E and J. Measurements in fluid environment were performed by using a MTFML cell (Veeco Metrology, Inc.). Samples imaged in air were scanned by using either silicon nitride RTESP probes (Veeco Instruments) with 40 N/m elastic constant and 300 kHz resonance frequency or silicon nitride, gold coated NSG01 probes (NT-MDT Co., Moscow, Russia) with 5.5 N/m elastic constant and 150 kHz resonance frequency. Imaging in fluid environment was performed by using silicon NP-S probes (Veeco Metrology, Inc.) with 0.58 N/m elastic constant and 30 kHz resonance frequency.

Samples for air operation AFM were prepared by depositing 10 μ L of the tetrapeptide solution in 50 mM acid phosphate buffer (pH 3.5) on freshly cleaved muscovite mica or pyrolytic graphite. After 25 s of deposition, samples were washed 3 times with 50 μ L of ultra-pure water to remove buffer and non adherent tetrapeptide. For fluid operation imaging, a cell was inserted over the sample holder containing a mica substrate. The cell was filled with a solution of 3 mM RVDV in ultra-pure water.

The RWDW hydrogel was prepared by adding 0.15 mL of 0.1 M NaOH solution to 1.3 mL of 14.5 mM RWDW water solution containing 0.35% CaCl_2 .

Results and discussion

The two studied tetrapeptides, RWDW and RVDV, differ for the structure of the neutral hydrophobic residue, as they contain two tryptophan and two valine residues, respectively (Fig. 1).

The critical aggregation concentration (cac) was initially evaluated by light scattering measurements on tetrapeptide solutions having concentrations between 10 μ M and 10 mM. The scattered light increased considerably at concentrations above 0.4 and 3 mM for RWDW and RVDV, respectively (Fig. 2), showing a greater tendency to aggregation by RWDW.

Viscosity measurements were employed to confirm the cac of the tetrapeptides and to evaluate the kinetics of the phenomenon. To guarantee the reproducibility of the measurements and to avoid the presence of dust specks that could clog the viscometer capillary, the stock solution was filtered at 5 μ m. In order to verify that the filtration procedure did not appreciably modify the oligopeptide concentration, the UV-Vis absorption spectrum of a RWDW solution close to the cac was recorded before and after the filtration (Fig. 3). The absorbance of the filtered sample was slightly lower than that of the raw sample; this behavior may be due to the retention of tetrapeptide aggregates larger than the size of filter pores or to oligopeptide adsorption by the filter. In any case, the concentration reduction, being within 5%, can be neglected.

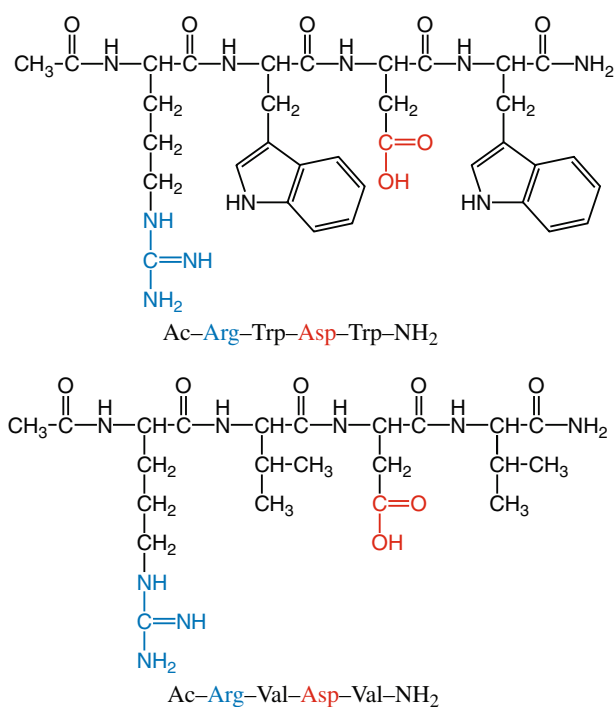


Fig. 1 Structures of RWDW and RVDV tetrapeptides

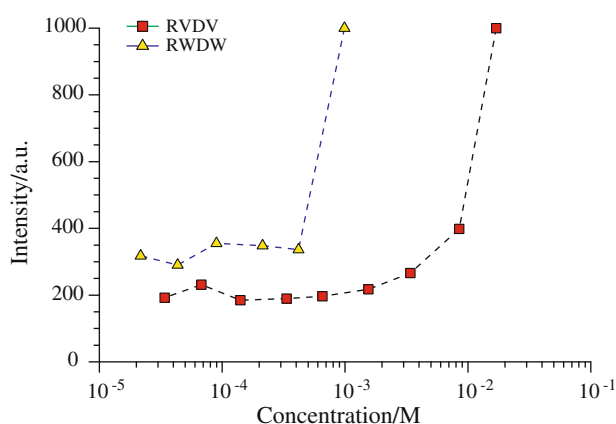


Fig. 2 Dependency of scattered light intensity on tetrapeptide concentration in 50 mM phosphate buffer at pH 3.5

To study the self-assembly kinetics, as soon as the capillary was loaded with RWDW solution, the specific viscosity (η_{sp}) was monitored versus time. The solution viscosity increased for about 2 h before reaching an equilibrium value, although the major changes occurred within 30 min (data not shown). This behavior indicates that the self-assembling process is quite slow; accordingly, all measurements were performed 2 h after the sample preparation. The plots of RWDW and RVDV specific viscosity versus tetrapeptide concentration show a slope variation around 0.5 and 2.0 mM, respectively (Fig. 4), which can be associated to the formation of oligopeptide fibrils. Indeed,

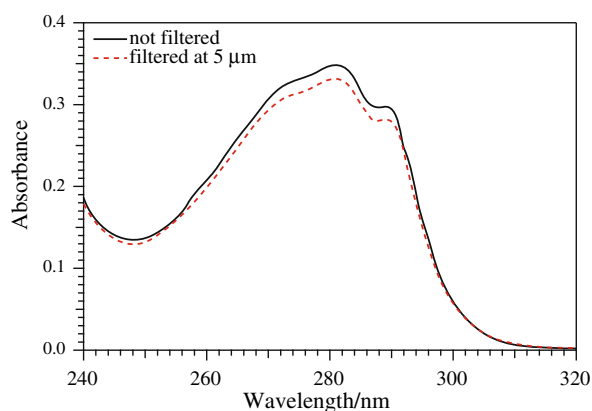


Fig. 3 UV-vis absorption spectra of 0.42 mM solution of RWDW in phosphate buffer 50 mM at pH 3.5, before and after filtration

viscosity is particularly affected by the presence of long fibrils in solution. Moreover, the η_{sp} of RVDV solutions is definitely lower than that of RWDW solutions of comparable concentration. These data not only demonstrate the lower tendency of RVDV to aggregate but also its lower capacity to form long fibrils, which are those that most influence viscosity.

AFM images of the tetrapeptides cast on mica from phosphate buffer solution show aggregates, whose number

Fig. 4 Specific viscosity of RWDW (*left*) and RVDV (*right*) in phosphate buffer solution (50 mM, pH 3.5)

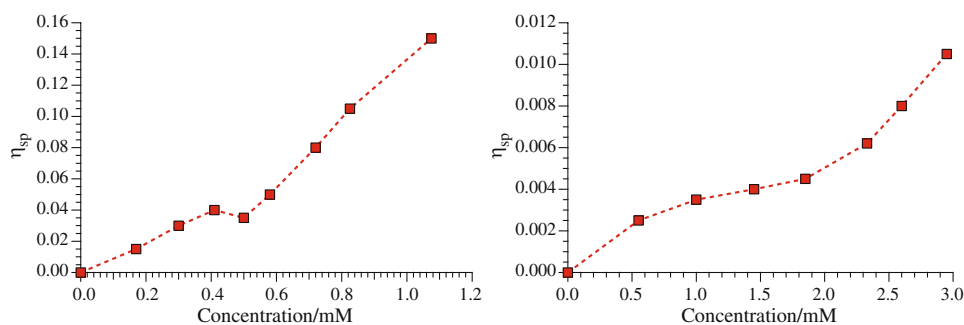
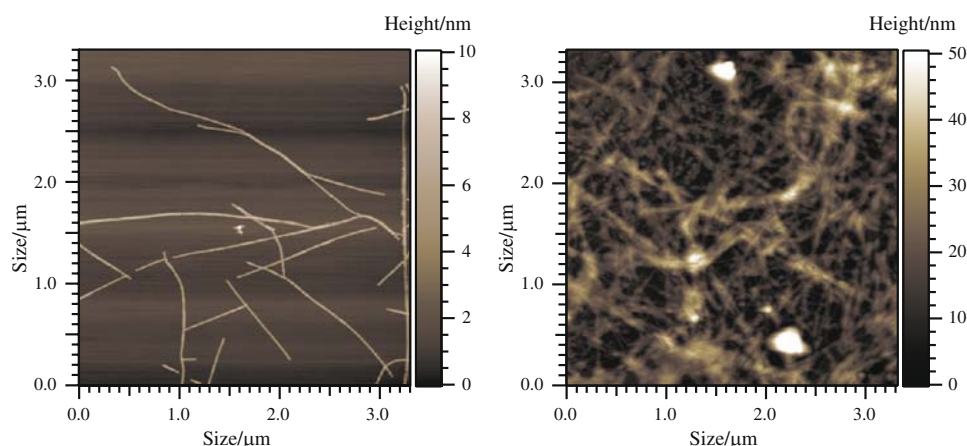


Fig. 5 AFM topography of RWDW cast on mica from 0.47 mM (*left*) and 1.04 mM (*right*) solutions in 50 mM pH 3.5 phosphate buffer



and length increase with increasing oligopeptide concentration. RWDW forms long fibrils around the cac (0.47 mM), and a network of long intertwined fibrils at higher (1.04 mM) oligopeptide concentration (Fig. 5). RWDW presented a similar behaviour when cast on pyrolytic graphite (Fig. 6).

The cross-sections of oligopeptide fibrils cast on either mica or graphite are compared in Fig. 7. Thickness and width of fibrils were evaluated to be about 4.0–4.5 and 40–60 nm, respectively. The similarity in morphology and size indicate that the interaction with substrate only has a minor influence on the formation process of fibrils. Aggregates are assembled in solution and then stick to the substrate, thanks to the interaction among already formed fibrils and the surface [10].

An analogous behaviour was observed when a 10 mM solution of RVDV in 50 mM pH = 3.5 phosphate buffer was deposited on mica, even if the morphology of the fibre network was less regular. Also in this case experiments performed on pyrolytic graphite led to the formation of similar fibrillar aggregates. In particular, AFM images highlighted the in situ formation of fibrils and planar aggregates with thickness of 2 and 1.1 nm, respectively. One can speculate that the fibres are constituted by a double molecular layer whereas planar aggregates consist of a monolayer.

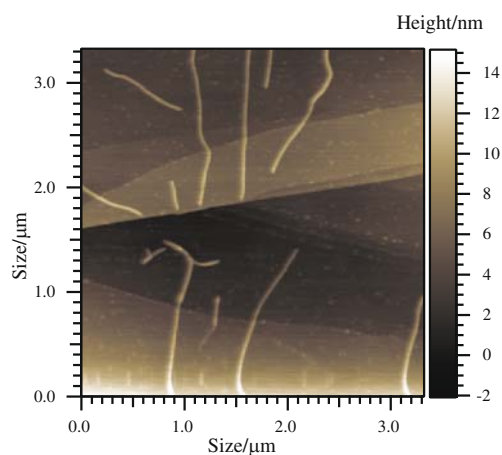


Fig. 6 AFM topography of RWDW cast on pyrolytic graphite from 0.47 mM solution in 50 mM pH 3.5 phosphate buffer

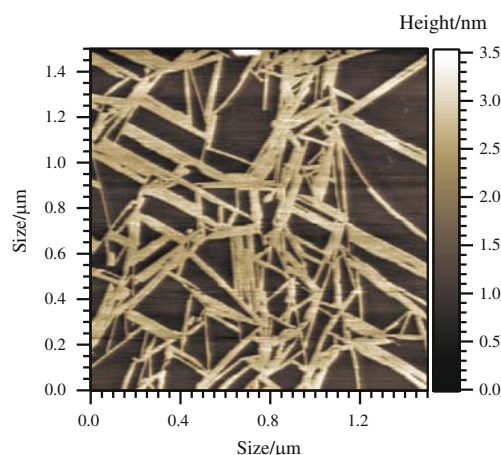


Fig. 8 AFM topography in liquid of the mica surface in contact with 3 mM RVDV water solution

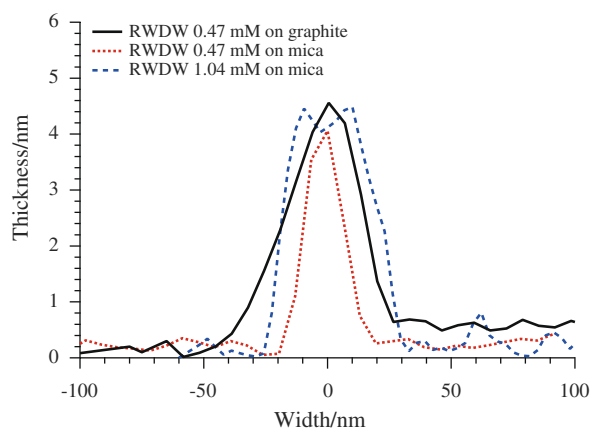


Fig. 7 Comparison of the transverse cross-section of RWDW fibrils

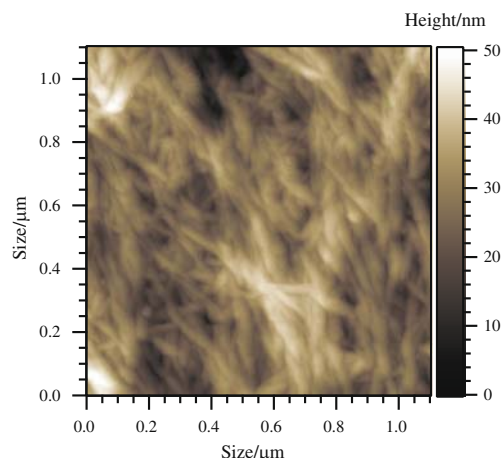


Fig. 9 AFM topography of dried RWDW hydrogel cast on mica substrate

Imaging in liquid was performed on RVDV solutions in ultra-pure water placed on mica. The sample was imaged 25 min after the deposition. Also in this case, AFM images highlighted the in situ formation of fibrils and planar aggregates with thickness of about 2 nm (Fig. 8). This result demonstrates that at least at the examined concentrations, the planar structures observed in liquid environment consist of fibrils placed side by side.

It was found that at high concentration (above the *cac*), RWDW tends to form transparent gels in phosphate buffer solution at pH 7.4 and in neutral solutions containing CaCl_2 . The AFM images of the dried gel, formed in a neutralized CaCl_2 solution, show a “spaghetti” type assembly (Fig. 9). The various performed experiments lead to assert that the presence of charged residues on the tetrapeptide, as well as salts in solution play an important role in the self-assembly process, as already reported in literature [11]. The study of the gelation conditions will be particularly interesting for tissue engineering applications.

The thermodynamic parameters associated with the self-aggregation of surfactant, biological detergents and polymers can be obtained from isothermal titration calorimetry (ITC) [12, 13]. ITC, at best of our knowledge, has not been employed until now to study the self-assembly of short oligopeptides. Indeed, the heat effects of intra- and intermolecular processes in dilute solutions are extremely small. In this study, ITC was used as an additional technique to investigate the aggregation behavior of RWDW in phosphate buffer solution.

The titrations consisted of sequential injections of highly concentrated tetrapeptide solution. Each injection induced a heat flow as a function of time and by its integration the ΔH_{inj} was obtained. With increasing oligopeptide concentration in the sample cell, the heat flow decreased and became constant (almost zero) at the end of the experiment. The heat effect of each injection was generally quite small thus making rather difficult the peak integration.

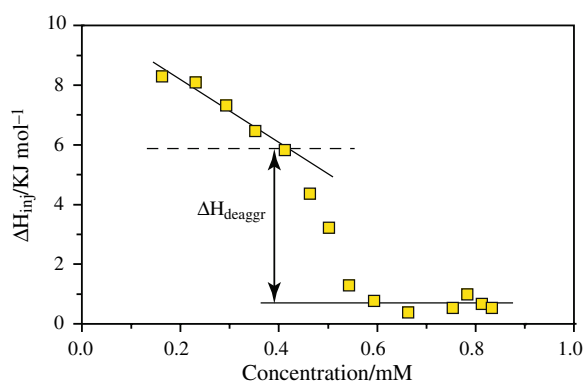


Fig. 10 Typical dilution enthalpogram of a RWDW solution

Table 1 Comparison of cac as determined by using different techniques

Technique	RWDW (mM)	RVDV (mM)
Light scattering	0.4 ± 0.1	3 ± 0.5
Viscosimetry	0.5 ± 0.1	2 ± 0.6
ITC	0.5 ± 0.04	ND

Accordingly, each titration was performed three times to guarantee the reproducibility of the results.

The enthalpograms of RWDW solutions resulted in sigmoidal calorimetric dilution curves (Fig. 10), thus revealing that the aggregation process is cooperative [14]. The recorded data showed that the heat effects per injection are endothermic, implying that the deaggregation process is endothermic as well. Analysis of the sigmoidal dilution curve allows for evaluating a $\Delta H_{deaggr} = 4.9 \pm 0.5$ kJ/mol.

The cac (0.5 mM) was easily determined by calculating the first derivative of the ΔH_{inj} with respect to the tetrapeptide concentration in the cell. The results obtained by microcalorimetry are consistent with light scattering and viscosimetry measurements; indeed the cac are of the same order of magnitude (Table 1).

In the case of the RVDV tetrapeptide, the heat effect per injection was too small for reliable integration and hence neither cac nor ΔH_{deaggr} could be determined suggesting that a more sensitive calorimeter is needed to study the thermodynamics of RVDV self-assembly.

Conclusions

The reported results indicate that the self-assembly of self-complementary ionic tetrapeptides is strongly related to the hydrophobicity of side-chains. Indeed, a larger hydrophobicity favours the mutual contact among molecules by excluding water molecules. However further investigations

are needed in order to deepen the influence of the secondary structure of the oligopeptides on the self-assembly process.

AFM imaging clearly showed the presence of fibrils only at concentrations higher than cac . Moreover, the tetrapeptide concentration did not affect fibril width and thickness: peptide addition only resulted in an increase of fibril length and number. Almost the same aggregate morphology was observed both on hydrophilic mica and hydrophobic graphite. This behaviour clearly demonstrates that the self-assembly process occurs in solution and is appreciably not affected by the interactions of the tetrapeptide with the substrate whose nature can however favour fibril adhesion.

Acknowledgements The financial support by MIUR FIRB 2003 project and Fondazione Cassa di Risparmio di Pisa is gratefully acknowledged.

References

- Zhang S, Altman M. Peptide self-assembly in functional polymer science and engineering. *React Func Polym.* 1999;41:91–102.
- Walsh DM, Hartley DM, Kusumoto Y, Fezoui Y, Condron MM, Lomakin A, et al. Amyloid β -protein fibrillogenesis structure and biological activity of protofibrillar intermediates. *J Biol Chem.* 1999;274:25945–52.
- Zhang S. Emerging biological materials through molecular self-assembly. *Biotechnol Adv.* 2002;20:321–39.
- Holmes TC. Novel peptide-based biomaterial scaffolds for tissue engineering. *Trends Biotechnol.* 2002;20:16–21.
- Zhang S, Holmes TC, Lockshin C, Rich A. Spontaneous assembly of a self-complementary oligopeptide to form a stable macroscopic membrane. *Proc Natl Acad Sci USA.* 1993;90:3334–8.
- Zhang S, Rich A. Direct conversion of an oligopeptide from a β -sheet to an α -helix: a model for amyloid formation. *Proc Natl Acad Sci USA.* 1997;94:23–8.
- Stine WB, Dahlgren KN, Krafft GA, Ladu ML. In vitro characterization of conditions for amyloid- β peptide oligomerization and fibrillogenesis. *J Biol Chem.* 2003;278:11612–22.
- Duce C, Monti S, Solaro R, Tiné MR. Ionic peptide aggregation: exploration of conformational dynamics in aqueous solution by computational techniques. *J Phys Chem B.* 2007;111:1165–75.
- Monti S, Alderighi M, Duce C, Solaro R, Tiné MR. Adsorption of ionic peptides on inorganic supports. *J Phys Chem C.* 2009;113:2433–42.
- Yang H, Fung S, Pritzker M, Chen P. Modification of hydrophilic and hydrophobic surfaces using an ionic-complementary peptide. *PLoS ONE.* 2007;12:1–11.
- Hennick WE, Van Nostrum CF. Novel crosslinking methods to design hydrogels. *Adv Drug Deliv Rev.* 2002;54:13–36.
- Garidel P, Hildebrand A. Thermodynamic properties of association colloids. *J Therm Anal Cal.* 2005;82:483–9.
- Raju BB, Winnik FM, Morishima Y. A look at the thermodynamics of the association of amphiphilic polyelectrolytes in aqueous solutions: strengths and limitations of isothermal titration calorimetry. *Langmuir.* 2001;17:4416–21.
- Kljin JE, Kevelam J, Engberts JBFN. Aggregation behavior of mono-encapped hydrophobically modified poly(sodium acrylate)s in aqueous solution. *J Coll Interf Sci.* 2000;226:76–82.